



# Isoflurane modulates cardiac mitochondrial bioenergetics by selectively attenuating respiratory complexes

Bhawana Agarwal<sup>a</sup>, Ranjan K. Dash<sup>b,c,d</sup>, David F. Stowe<sup>a,b,d,e,f</sup>, Zeljko J. Bosnjak<sup>a,b,d</sup>, Amadou K.S. Camara<sup>a,d,\*</sup>

<sup>a</sup> Department of Anesthesiology, Medical College of Wisconsin, Milwaukee, WI, USA

<sup>b</sup> Department of Physiology, Medical College of Wisconsin, Milwaukee, WI, USA

<sup>c</sup> Biotechnology and Bioengineering Center, Medical College of Wisconsin, Milwaukee, WI, USA

<sup>d</sup> Cardiovascular Research Center, Medical College of Wisconsin, Milwaukee, WI, USA

<sup>e</sup> Research Service, Zablocki VA Medical Center, Milwaukee, WI, USA

<sup>f</sup> Department of Biomedical Engineering, Marquette University, Milwaukee, WI, USA

## ARTICLE INFO

### Article history:

Received 5 July 2013

Received in revised form 28 October 2013

Accepted 13 November 2013

Available online 17 December 2013

### Keywords:

Volatile anesthetic

Isoflurane

Mitochondrial bioenergetics

Electron transport chain

Cardiac IR injury

Cardioprotection

## ABSTRACT

Mitochondrial dysfunction contributes to cardiac ischemia–reperfusion (IR) injury but volatile anesthetics (VA) may alter mitochondrial function to trigger cardioprotection. We hypothesized that the VA isoflurane (ISO) mediates cardioprotection in part by altering the function of several respiratory and transport proteins involved in oxidative phosphorylation (OxPhos). To test this we used fluorescence spectrophotometry to measure the effects of ISO (0, 0.5, 1, 2 mM) on the time-course of interlinked mitochondrial bioenergetic variables during states 2, 3 and 4 respiration in the presence of either complex I substrate K<sup>+</sup>-pyruvate/malate (PM) or complex II substrate K<sup>+</sup>-succinate (SUC) at physiological levels of extra-matrix free Ca<sup>2+</sup> (~200 nM) and Na<sup>+</sup> (10 mM). To mimic ISO effects on mitochondrial functions and to clearly delineate the possible ISO targets, the observed actions of ISO were interpreted by comparing effects of ISO to those elicited by low concentrations of inhibitors that act at each respiratory complex, e.g. rotenone (ROT) at complex I or antimycin A (AA) at complex III. Our conclusions are based primarily on the similar responses of ISO and titrated concentrations of ETC inhibitors during state 3. We found that with the substrate PM, ISO and ROT similarly decreased the magnitude of state 3 NADH oxidation and increased the duration of state 3 NADH oxidation,  $\Delta\Psi_m$  depolarization, and respiration in a concentration-dependent manner, whereas with substrate SUC, ISO and ROT decreased the duration of state 3 NADH oxidation,  $\Delta\Psi_m$  depolarization and respiration. Unlike AA, ISO reduced the magnitude of state 3 NADH oxidation with PM or SUC as substrate. With substrate SUC, after complete block of complex I with ROT, ISO and AA similarly increased the duration of state 3  $\Delta\Psi_m$  depolarization and respiration. This study provides a mechanistic understanding in how ISO alters mitochondrial function in a way that may lead to cardioprotection.

© 2013 Published by Elsevier B.V.

## 1. Introduction

Mitochondria are primary mediators of cardiac ischemia–reperfusion (IR) injury [1–4]; they are also important targets for volatile anesthetic (VA)-induced cardioprotection against IR injury [3,5–12]. Cardioprotection by a VA can be instituted either before the onset of ischemia (anesthetic pre-conditioning: APC) or at the onset of reperfusion (anesthetic post-conditioning: APOC) [13,14]. Regardless of the cardioprotective strategy, VAs exert effects on mitochondrial function.

Mitochondrial failure consequent to bioenergetic dysfunction leads to cell damage during IR but specific components of the mitochondrial bioenergetic mechanisms may be targets for the actions of VAs that underlie APC or APOC against IR injury. Volatile anesthetics, including isoflurane (ISO) are known to mediate cardioprotection against IR injury, in part, by attenuating function of the electron transport chain (ETC) protein complex I (NADH oxidoreductase) and by triggering mild

ROS production, a critical mediator for cellular protection [15–18]. The mechanisms of ISO and other VAs to alter mitochondrial function and confer cardioprotection via their actions on ETC complexes and other mitochondrial transport proteins, however, are not well understood.

It may seem incongruous at first that IR-induced injury ultimately leads to dysfunction of mitochondrial respiration but, on the other hand, attenuation of mitochondrial respiration might minimize mitochondrial injury and reduce cell death during cardiac IR injury [19,20]. Thus, an understanding of ISO-induced actions on selective mitochondrial proteins, including the ETC complexes and transport proteins that are crucial for oxidative phosphorylation (OxPhos), is essential in elucidating the mechanisms of ISO-induced cardioprotection against IR injury.

In our recent study in isolated mitochondria [8] in which we demonstrated that ISO attenuates Ca<sup>2+</sup> extrusion by the mitochondrial Na<sup>+</sup>/Ca<sup>2+</sup> exchanger, we also found that ISO caused a concentration-dependent decrease in the rate of state 3 NADH oxidation and ADP phosphorylation with the complex I substrate pyruvate/malate (PM).

\* Corresponding author.

Complex I was first suggested as a site for VA effects [21,22]; this was supported by later findings [23,24]. Our initial observed effects of ISO [8] to increase the duration of state 3 NADH oxidation and  $\Delta\Psi_m$  depolarization also supported complex I as a site of action, but this could alternatively have been due to inhibition of other ETC. complexes downstream of complex I, e.g., complexes III (ubiquinol cytochrome c oxidoreductase), IV (cytochrome c oxidase) and V ( $F_1F_0$  ATP synthase), or complex II (succinate dehydrogenase) and transport proteins (e.g. adenine nucleotide transporter, ANT); alternatively, as has been reported, ISO might act as an uncoupling agent by promoting a proton leak [25] that could lead to mild  $\Delta\Psi_m$  depolarization.

Because our understanding of the mechanisms of ISO-targeted mitochondrial interventions is not well defined, we compared the ISO effects to those elicited by low concentrations of known site-specific inhibitors of mitochondrial proteins. That is, we explored the potential mitochondrial targets of ISO by comparing its concentration-dependent effects with the concentration-dependent effects of known inhibitors of ETC. complexes and mitochondrial transport proteins to identify, and also rule out, possible ISO targets. In this way we hoped to better understand how VA-induced modification of mitochondrial bioenergetics can contribute to cardioprotection. To carry out our aims we used isolated cardiac mitochondria energized with substrates  $K^+$ -pyruvate/malate (PM),  $K^+$ -succinate (SUC) or SUC + Rotenone (ROT, 1  $\mu$ M). Low concentrations of ROT antimycin A (AA), oligomycin (OMN), and atractyloside (ATR) were used to stepwise attenuate complexes I, III, V and ANT function, respectively; low concentrations of malonate (MAL) and potassium cyanide (KCN) were used in some experiments to attenuate functions of complexes II and IV, respectively.

## 2. Materials and methods

### 2.1. Mitochondrial isolation

Mitochondria were freshly isolated from hearts of Wistar rats (300–350 g) using protocols approved by the Medical College of Wisconsin Institutional Animal Care and Use Committee (IACUC) as described previously [8]. Briefly, rats were anesthetized with an intraperitoneal injection of inactin (150 mg/kg), and the ventricles were excised and placed in an ice-cold isolation buffer that contained (in mM): 200 mannitol, 50 sucrose, 5  $KH_2PO_4$ , 5 MOPS, 1 EGTA and 0.1% BSA, with pH adjusted to 7.15 with KOH. The ventricles were minced in the presence of 5 U/ml protease (*Bacillus licheniformis*, Sigma) followed by differential centrifugation. All isolation procedures were carried out at 4 °C. Mitochondrial protein content was determined by the Bradford method [26]. The final mitochondrial pellet was resuspended in isolation buffer and kept on ice. All chemicals were procured from Sigma (St. Louis, MO, USA), unless stated otherwise.

### 2.2. Measure of mitochondrial redox state (NADH)

NADH autofluorescence was measured in the mitochondrial suspension during states 2, 3 and 4 respiration using fluorescence spectrophotometry at excitation wavelength 350 nm and emission wavelengths 395 nm and 456 nm (Photon Technology International, Birmingham, NJ), as we have described before [8,27–30]. At the end of each experiment (390 s), maximal (fully reduced) NADH (high NADH/NAD<sup>+</sup>) was determined with 1  $\mu$ M ROT, which completely blocks electron transport via FeS centers in complex I at the ubiquinone (Q) binding site so that proton pumping from NADH cannot occur; minimal (fully oxidized) NADH (low NADH/NAD<sup>+</sup>) was determined with 20  $\mu$ M trifluorocarbonyl cyanide phenylhydrazone (FCCP), which induces maximal proton leak, and causes an increase in proton pumping and electron transfer between ETC complexes. The ratio of emission fluorescence (456/395) was normalized between the fully oxidized (with FCCP) state to the fully reduced (with ROT) state to represent % NADH as the total pool of NADH + NAD<sup>+</sup>.

### 2.3. Measure of mitochondrial membrane potential ( $\Delta\Psi_m$ )

$\Delta\Psi_m$  was measured in the mitochondrial suspension during states 2, 3 and 4 respiration by fluorescence spectrophotometry using the fluorescent dye tetramethyl-rhodamine methyl ester (1  $\mu$ M TMRM; Molecular Probes, Eugene, OR) at excitation wavelengths 546 nm and 573 nm and emission wavelength 590 nm [31], as we have described [29]. TMRM is a ratiometric, membrane potential sensitive, cationic fluorophore that equilibrates across the inner mitochondrial membrane (IMM) based on its electrochemical potential.  $\Delta\Psi_m$  measurements followed the same time-line protocol as NADH measurements except that the respiratory uncoupler carbonyl cyanide *m*-chlorophenylhydrazone (4  $\mu$ M CCCP) was used to fully depolarize  $\Delta\Psi_m$ . The ratio of excitation wavelengths (546/573) at any time point was plotted as a percent of maximum fluorescence (100%) obtained by maximal depolarization with CCCP.

### 2.4. Measure of mitochondrial O<sub>2</sub> consumption

Mitochondrial O<sub>2</sub> consumption rate (respiration) was measured using a Clark-type O<sub>2</sub> electrode (System S 200A; Strathkelvin Instruments, Glasgow, UK) as we have described before [8,30,32,33]. Functional integrity of mitochondria was determined by the respiratory control index (RCI), defined here as the ratio of state 3 (after added ADP) to state 4 respiration (after complete phosphorylation of the added ADP). Only mitochondrial preparations with RCI  $\geq$  6, measured with PM, were used to conduct further experiments.

### 2.5. Protocol

Measures of the three bioenergetic variables (NADH,  $\Delta\Psi_m$ , and respiration) were conducted with mitochondria (0.5 mg/ml) suspended in respiration buffer that contained (in mM): 130 KCl, 10 NaCl, 0.5  $CaCl_2$ , 5  $K_2HPO_4$ , 20 MOPS, 1 EGTA and 0.1% BSA at pH 7.15 adjusted with KOH, at room temperature (25 °C). NADH,  $\Delta\Psi_m$ , and respiration were monitored under complex I-linked substrate (10 mM PM) or complex II-linked substrate (10 mM SUC) during respiratory states 2 (before adding ADP), 3 (during phosphorylation of 250  $\mu$ M ADP), and 4 (after complete phosphorylation of the ADP). Along with drug free controls (0.1% DMSO), either of three concentrations of ISO (0.5, 1, 2 mM) or several titrated low concentrations of respiratory complex inhibitors (e.g. 30, 50, 80, 120, 150 nM ROT; 25, 75, 85, 100, 110 nM AA) were added to the buffer after adding the substrate, followed by ADP. All drugs were dissolved in DMSO (0.1%). The appropriate volumes of ISO stock solutions dissolved in DMSO were prepared in tightly sealed glass vials and specific volumes from these vials were added to the experimental buffer (1 ml) to obtain the desired ISO concentrations (i.e. 0.5, 1 and 2 mM). ISO, 0.5 mM, is equivalent to approximately 1.4% atm at 25 °C with an estimated 1.3 minimum alveolar concentration (MAC) for rats [23]. To confirm the actual concentrations of ISO in each mitochondrial suspension, an aliquot of isoflurane in solution from each vial was obtained and measured by gas chromatography at the beginning (100 s) and end of each experiment (500 s). For added ISO, the measured values varied within  $\pm$  10% of their initial prepared values of 0.5, 1, 1.5 and 2 mM. The time-course protocol consisted of the following: (1) 0 s, addition of mitochondrial sample into the respiration buffer and start of recording; (2) 30 s, introduction of the substrate (PM or SUC or SUC + ROT) (1  $\mu$ M; high concentration that completely blocks electron flow from complex I) (state 2); (3) 90 s, addition of either of DMSO, ISO or other mitochondrial protein inhibitors, and (4) 150 s, addition of ADP (state 3).

Adding substrate PM or SUC provided for forward electron transfer from complex I or II through complex IV, respectively, and only reverse electron transfer from complex II to I with SUC. Substrate SUC with a complete block of complex I by ROT (1  $\mu$ M) allowed for forward electron transfer only from complex II through IV. Sites of inhibition by

blockers of each of the five respiratory complexes, and ANT, as well as how modulation of  $\Delta\Psi_m$  and matrix pH are all involved in OxPhos are shown schematically (Fig. 1).

## 2.6. Data analysis and statistics

Traces are representative of the mean of three different mitochondrial preparations, each with three replicate recordings. Where appropriate, data are represented as mean  $\pm$  SD of three independent experiments. All data were compiled using Microsoft Excel and analyzed using one-way ANOVA (analysis of variance) with Turkey's post-hoc test for significance of means. Differences with  $P < 0.05$  (two-tailed) were considered significant.

## 3. Results

### 3.1. Effect of isoflurane vs. respiratory inhibitors on mitochondrial redox state (NADH)

Time-dependent effects of DMSO (vehicle) and graded concentrations of ISO, complex I (ROT), or complex III (AA) inhibitors in the presence of the substrate PM or SUC during states 2, 3 and 4 are shown in Fig. 2A–F. The insets show summaries of their effects on the duration of ADP-induced state 3 NADH oxidation (S3 time, s). ISO, ROT, and AA each had no effect on resting state 2 NADH. With the complex I substrate PM, ISO caused pronounced concentration-dependent decreases in state 3 NADH oxidation with respect to state 2 NADH after adding ADP:  $32 \pm 7\%$ ,  $27 \pm 5\%$  and  $21 \pm 5\%$  at 0.5, 1 and 2 mM ISO, respectively, vs.  $42 \pm 4\%$  with DMSO. ISO also significantly increased the duration of state 3 NADH oxidation:  $50 \pm 4$  s,  $66 \pm 6$  s and  $103 \pm 8$  s at 0.5, 1 and 2 mM, respectively, vs.  $41 \pm 5$  s for DMSO (Fig. 2A inset).

To deduce if ISO decreased state 3 NADH oxidation by an action on complex I, the changes in NADH induced by ISO during state 3 with substrate PM were compared to the effects of titrated, low concentrations of the complex I inhibitor ROT (Fig. 2B). These data showed, similar to ISO, that ROT attenuated the magnitude of state 3 NADH oxidation in a

concentration-dependent manner:  $35 \pm 5\%$ ;  $25 \pm 6\%$ ; and  $14 \pm 4\%$  at 20, 30 and 50 nM, respectively, vs.  $41 \pm 4\%$  for DMSO. Also like ISO, ROT caused a concentration-dependent increase in the duration of state 3 NADH oxidation (Fig. 2B inset).

To determine if ISO-induced increases in the duration of state 3 NADH oxidation might also result from reduced proton pumping and electron transfer downstream from complex I, NADH oxidation was assessed with titrated, low concentrations of the complex III blocker AA (see Fig. 1). AA caused concentration-dependent increases in the duration of state 3 NADH oxidation (Fig. 2C; inset), but unlike ISO and ROT, it did not decrease the magnitude of state 3 NADH oxidation. These data indicated that with PM as substrate, ISO decreased the extent and increased the duration of state 3 NADH oxidation similar to that of ROT, while it only increased the duration of state 3 NADH oxidation similar to that of AA. This indicated that both complexes I and III might be functional targets for ISO to retard restoration of the redox state (Fig. 7A).

To test if the ISO-induced changes in the extent and duration of state 3 NADH oxidation could also result from reduced inward translocation of ADP in exchange for ATP extrusion (Fig. 1), NADH oxidation was measured with low concentrations (0.25 to 1  $\mu$ M) of the ANT inhibitor, ATR. But, unlike ISO, ATR caused concentration-dependent decreases in both the extent and duration of state 3 NADH oxidation (data not shown); together these findings suggested that there was reduced ADP entry and availability during state 3 to oxidize NADH. The complex IV blocker KCN at low titrated concentrations (up to 1  $\mu$ M) did not exhibit effects similar to ISO on any of the mitochondrial bioenergetic variables with any substrate tested (data not shown).

We tested further if the prolonged effects of ISO on the duration of NADH oxidation with the substrate PM during state 3 were different from those elicited by the complex II substrate SUC (Fig. 2D) and how these responses compared with the effects of 30–150 nM ROT (Fig. 2E) or 100 and 125 nM AA (Fig. 2F). With the substrate SUC, adding ADP prolonged the duration of NADH oxidation substantially more than with the substrate PM (Fig. 2D vs. A). ISO tended to only slightly reduce the magnitude of oxidation but to markedly decrease the duration of

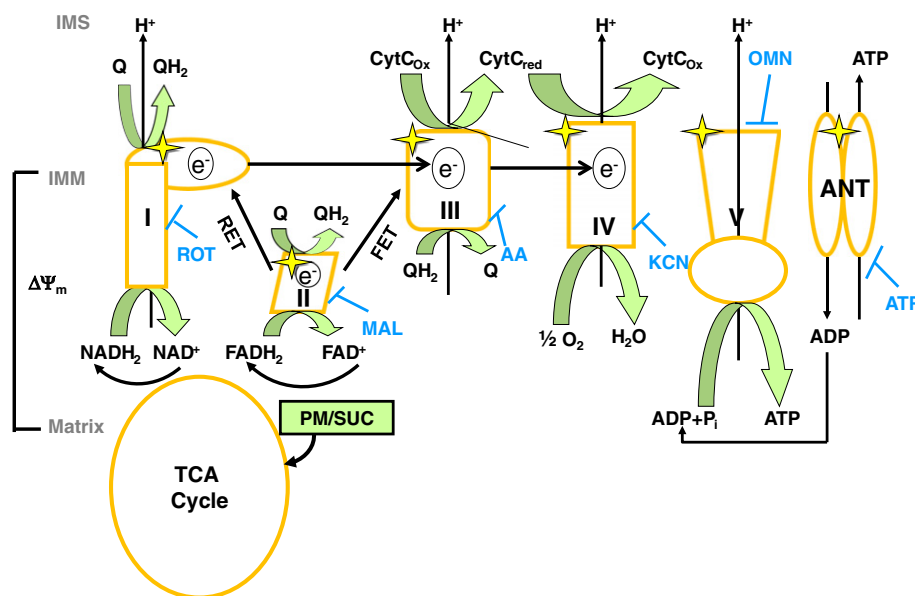


**Fig. 1.** Schema depicting the mitochondrial electron transport chain (ETC) protein complexes of the mitochondrial inner membrane (IMM), along with their specific inhibitors: rotenone (ROT), malonate (MAL), antimycin A (AA), potassium cyanide (KCN), oligomycin (OMN), and atractyloside (ATR). Reducing equivalents, NADH and FADH<sub>2</sub>, are generated via the tricarboxylic acid (TCA) cycle in the matrix, while electrons are transferred through the complexes to the final O<sub>2</sub> acceptor. At complex IV, coupled with this transfer is the pumping of protons (H<sup>+</sup>) into the intermembrane space (IMS) by complex I, complex III, and complex IV, which generate the H<sup>+</sup> gradient used by ATP synthase (complex V) to phosphorylate ADP to ATP. Depending on the substrate used, K<sup>+</sup>-pyruvate/malate (PM) or K<sup>+</sup>-succinate (SUC), isolated mitochondria respire differentially using NADH and FADH<sub>2</sub> to produce ATP; this is coupled to forward or reverse electron transfer (FET or RET) depending on the reduction potential across each complex and across the IMM. (⚡) represents potential targets of isoflurane (ISO) on the ETC components explored in this study.

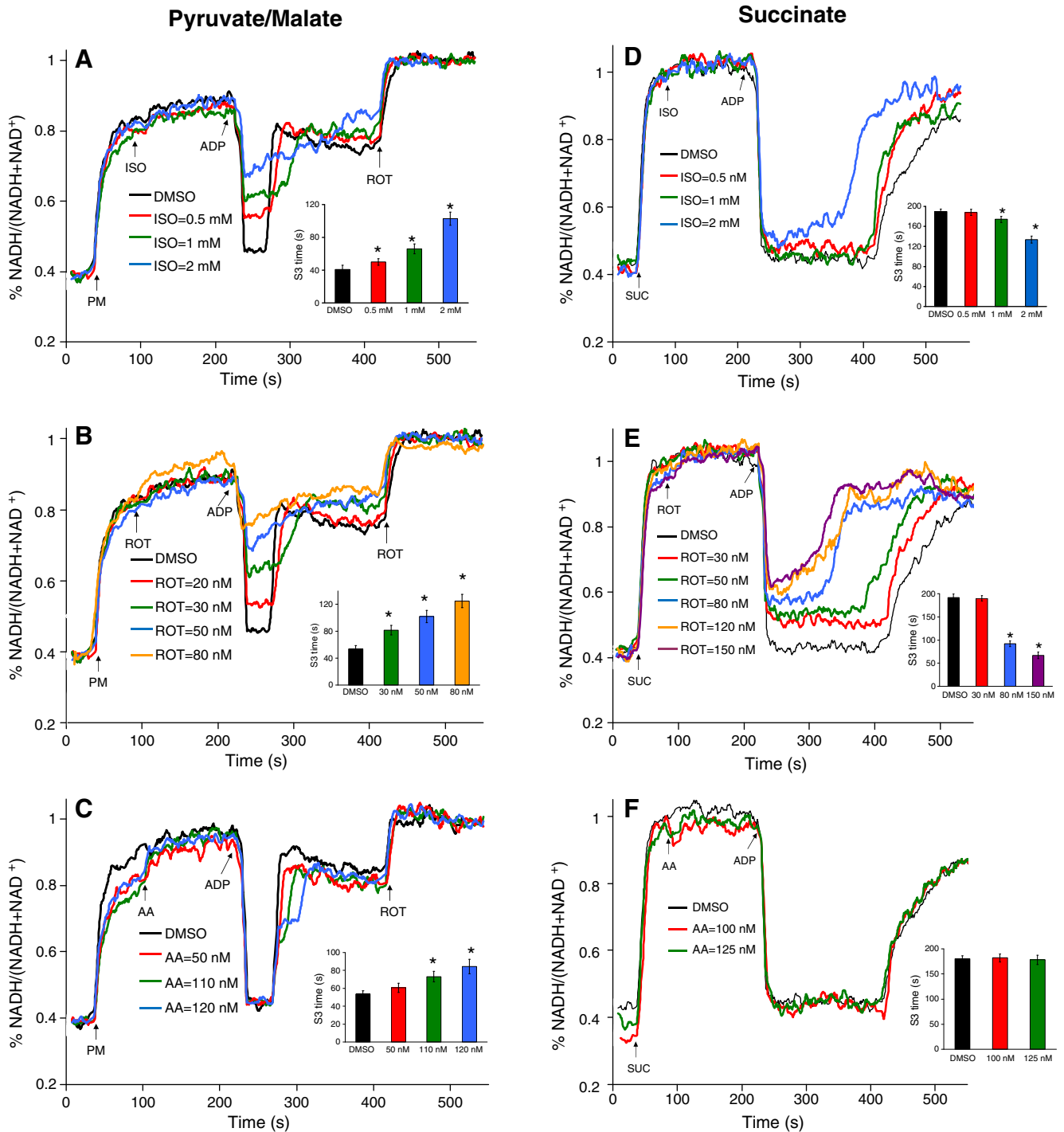


**Fig. 2.** Normalized mitochondrial redox state ( $\text{NADH}/(\text{NADH} + \text{NAD}^+)$ ) during states 2, 3 and 4 respiration with different substrates and either ISO or a blocker of ETC complexes. State 2 was induced with 10 mM PM (A–C) or SUC (D–F) and state 3 with 250  $\mu\text{M}$  ADP; state 4 is after phosphorylation of all ADP to ATP. ISO, ROT, or AA was added after PM or SUC and before ADP. ADP induced a transient decrease in the reduced state of NADH. The insets summarize effects of ISO compared to ROT and AA on duration of ADP-induced state 3 NADH oxidation (S3 time, s). Note similarities and differences of responses to each drug. NADH transients were normalized on a scale of 0–1, i.e. between fully oxidized to fully reduced states by adding excess FCCP or ROT, respectively. Data represent mean  $\pm$  SD of 3 replicates.

NADH oxidation (Fig. 2D inset). Because ROT attenuates both forward and reverse electron transfer through complex I, enhancing attenuation of proton pumping and electron transfer by ROT or ISO leads to less oxidation of NADH during state 3. ROT had a greater effect than ISO on both the extent and duration of NADH oxidation (Fig. 2E vs. D) suggesting that ISO may attenuate complex I function somewhat differently than ROT, which blocks electron transfer via a FeS centers at the Q

binding site in complex I. In contrast to the effects of ISO and ROT on attenuating state 3-induced oxidation of NADH with the substrate SUC, AA did not change the extent or duration of NADH oxidation (Fig. 2F) when compared to DMSO. Thus, these results suggested that ISO-induced effects on NADH redox state were mediated by attenuating complex I electron transfer, which in turn impeded proton pumping by NADH.



### 3.2. Effect of isoflurane vs. respiratory inhibitors on mitochondrial membrane potential ( $\Delta\Psi_m$ )

Time-dependent effects of DMSO (vehicle) and graded concentrations of ISO, complex I (ROT), or complex III (AA) inhibitors on  $\Delta\Psi_m$  in the presence of PM or SUC during respiratory states 2, 3 and 4 are shown in Fig. 3A–F. The insets show summaries of their effects on the

duration of ADP-induced depolarization of  $\Delta\Psi_m$  (S3 time, s). ISO, ROT and AA had no effect on resting state 2  $\Delta\Psi_m$ . Adding ADP caused a sudden, partial, and reversible  $\Delta\Psi_m$  depolarization in all groups because of the transiently smaller charge and pH gradients across the IMM due to the stimulation of respiration. With the complex I substrate, PM, ISO significantly increased the duration of state 3 depolarization of  $\Delta\Psi_m$ , i.e. by  $45 \pm 4$  s,  $81 \pm 7$  s and  $133 \pm 7$  s at 0.5, 1 and 2 mM,

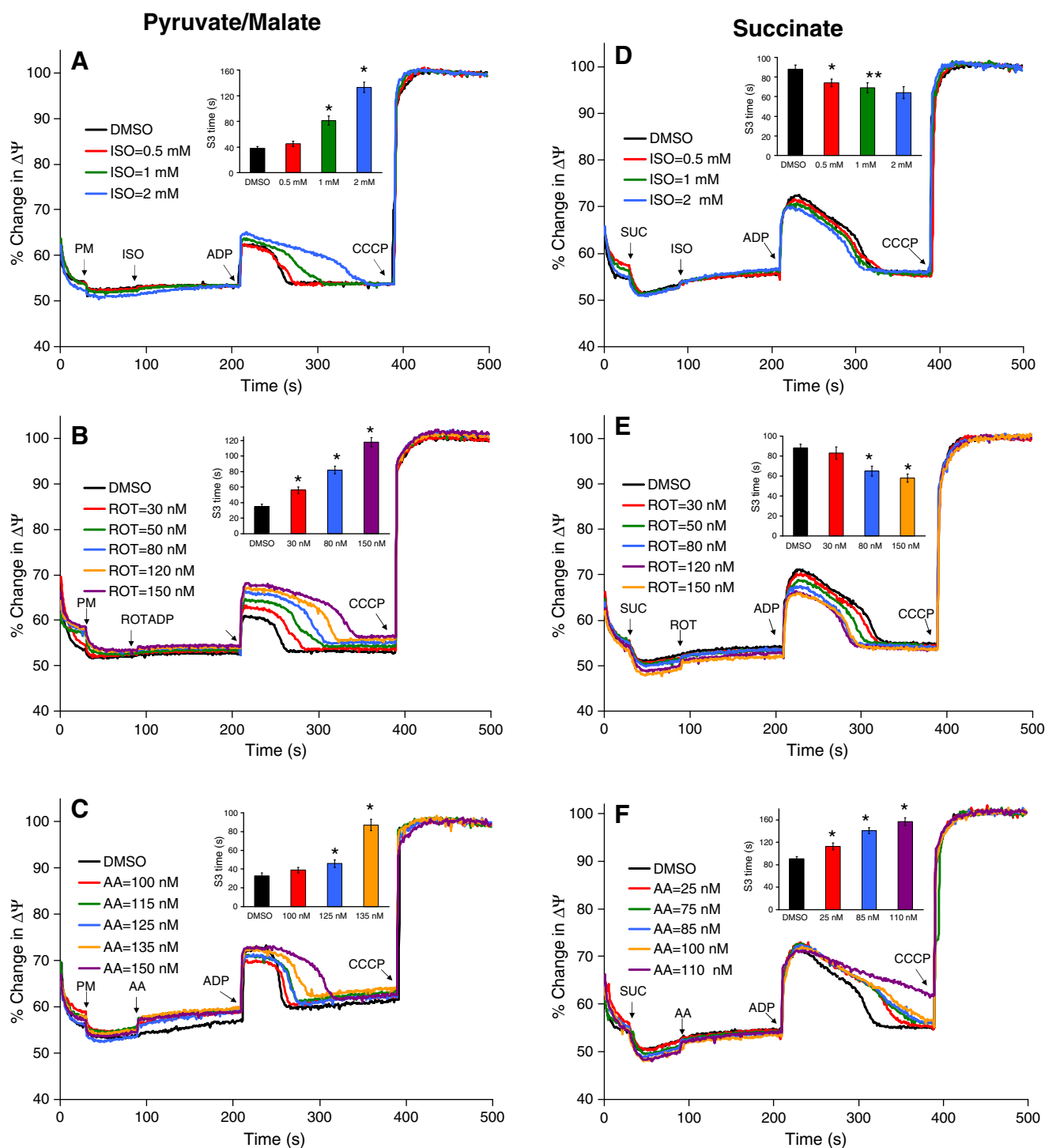


**Fig. 3.** Normalized mitochondrial membrane potential ( $\Delta\Psi_m$ ) during states 2, 3 and 4 respiration with different substrates and after adding either ISO or a blocker of ETC complexes. ISO, ROT, or AA was given after PM (A–C) or SUC (D–F), and before ADP, which induced a transient depolarization. The insets summarize effects of ISO compared to ROT and AA on duration of ADP-induced state 3 decreases in  $\Delta\Psi_m$  (S3 time, s). Note similarities and differences of responses to each drug.  $\Delta\Psi_m$  transients were normalized with respect to maximal (100%) depolarization obtained with added CCCP. Data represent mean  $\pm$  SD of 3 replicates.

respectively, vs.  $38 \pm 3$  s for DMSO (Fig. 3A). With the substrate PM, compared to DMSO, adding ADP after ISO, ROT, or AA caused a delay in state 3  $\Delta\Psi_m$  repolarization (Fig. 3A,B,C).

Like ISO, ROT had similar effects on the duration of state 3  $\Delta\Psi_m$  depolarization (Fig. 3A,B insets) and NADH oxidation (Fig. 2A,B insets) and on the increase in the magnitude of state 3  $\Delta\Psi_m$  depolarization; this was likely due to attenuation of complex I electron transfer and proton pumping during state 3. Like ISO (Fig. 3A inset), ROT and AA caused concentration-dependent increases in the duration of state 3  $\Delta\Psi_m$  depolarization (Fig. 3B,C insets). The observed ISO-induced increases in the extent and the duration of state 3  $\Delta\Psi_m$  depolarization (Fig. 3A) were consistent with the observed ISO-induced decrease in the extent and increase in the duration of state 3 NADH oxidation (Fig. 2A).

Unlike ISO with the substrate PM, and as observed with NADH, ATR (0.5–1  $\mu\text{M}$ ) caused a concentration-dependent attenuation of the ADP-induced decrease in  $\Delta\Psi_m$ , likely due to reduced ADP translocation through ANT (data not shown); Thus, the marked differences in ISO and ATR responses suggested again that the effects of ISO were not mediated via ANT.

Similar to the NADH measurements (Fig. 2), we also compared the effects of ISO, ROT, and AA (Fig. 3D,E,F), respectively, on changing the extent and duration of  $\Delta\Psi_m$  depolarization in the presence of the complex II substrate SUC during states 2, 3 and 4. ISO, ROT and AA had no effects on resting state 2  $\Delta\Psi_m$ . Adding ADP in the ISO and ROT groups caused small decreases in the magnitude of  $\Delta\Psi_m$  depolarization (Fig. 3D,E) and significant concentration-dependent decreases in the duration of state 3  $\Delta\Psi_m$  (Fig. 3D,E insets). In contrast, AA caused

concentration-dependent increases in the duration of ADP-induced  $\Delta\Psi_m$  depolarization (Fig. 3F and inset). The similarity of the concentration-dependent effects of ISO vs. ROT and AA (Fig. 3A–C) on the duration of the transient  $\Delta\Psi_m$  depolarization during state 3 duration (Fig. 3A inset) with NADH-linked substrate PM supports the notion that complexes I and III are targets for attenuated mitochondrial function by ISO. In contrast, giving AA in the presence of SUC did not mimic the effects of ISO on the duration of state 3  $\Delta\Psi_m$  depolarization (Fig. 3D vs. 3 F).

Because the state 3 effects on the duration of  $\Delta\Psi_m$  depolarization for ISO were similar to those of ROT, but somewhat dissimilar to AA in the presence of substrate SUC (Fig. 3D vs. E and F), we conducted additional experiments in which complex I was completely blocked by 1  $\mu\text{M}$  ROT before adding SUC; this was followed by addition of ISO or AA. Under these conditions both ISO and AA caused increases in the duration of ADP-induced  $\Delta\Psi_m$  depolarization, which re-affirmed that ISO has inhibitory effects on complex III (Fig. 4A,B). In this scenario it was likely that ISO, like AA, exerted similar effects to inhibit complex III when SUC was the substrate with complete inhibition of reverse electron transfer (RET) before adding SUC. When ISO (or AA) was added, the duration of  $\Delta\Psi_m$  depolarization increased because of slowed forward electron transfer (FET) to complex IV from complex III (Figs. 1, 7C). This slowing led to the increases in the duration of state 3  $\Delta\Psi_m$  depolarization.

However, it remained possible that ISO could also slow electron transport at complex II since this was another site of electron generation with SUC as the substrate. With complex I completely blocked by ROT, and SUC as the only substrate, adding the complex II inhibitor MAL

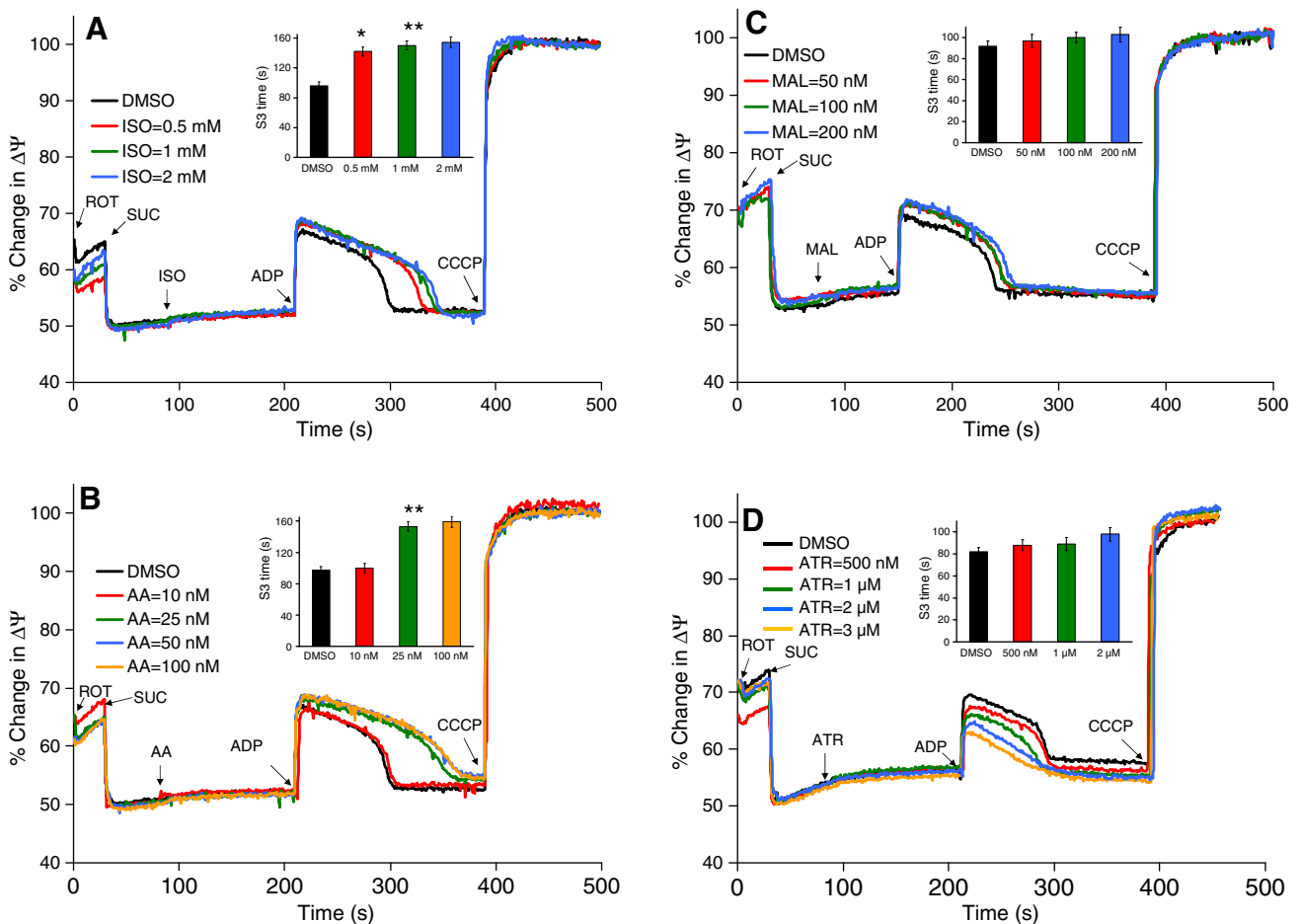


**Fig. 4.** Normalized mitochondrial membrane potential ( $\Delta\Psi_m$ ) during states 2, 3 and 4 respiration with SUC + ROT and either ISO or a blocker of ETC. ROT (1  $\mu\text{M}$ ) was given before other drugs to maximally block complex I. ISO (A), AA (B), MAL (C), or ATR (D) was added after SUC (A–D) and before adding ADP, which induced a transient depolarization. The insets summarize effects of ISO compared to AA, MAL, and ATR on duration of state 3 ADP-induced decreases in  $\Delta\Psi_m$  (S3 time, s). Note similarities and differences of responses to each drug.  $\Delta\Psi_m$  transients were normalized with respect to maximal (100%) depolarization obtained with added CCCP. Data represents mean  $\pm$  SD of 3 replicates.

(50–200 nM) resulted in only slight but not significant increases in maximal state 3  $\Delta\Psi_m$  depolarization (Fig. 4C) and state 3 duration (Fig. 4C inset). Because this is unlike the response of ISO to the increased state 3 duration, we concluded that ISO has no demonstrable effects on complex II.

We also examined if ANT is sensitive to ISO when complex I is first blocked by ROT before adding the substrate SUC. Under conditions of SUC + ROT (1  $\mu\text{M}$ ), ISO increased the duration of state 3  $\Delta\Psi_m$ ; therefore we explored the possibility that this may result in part from a decreased rate of ADP phosphorylation by attenuation of ANT for

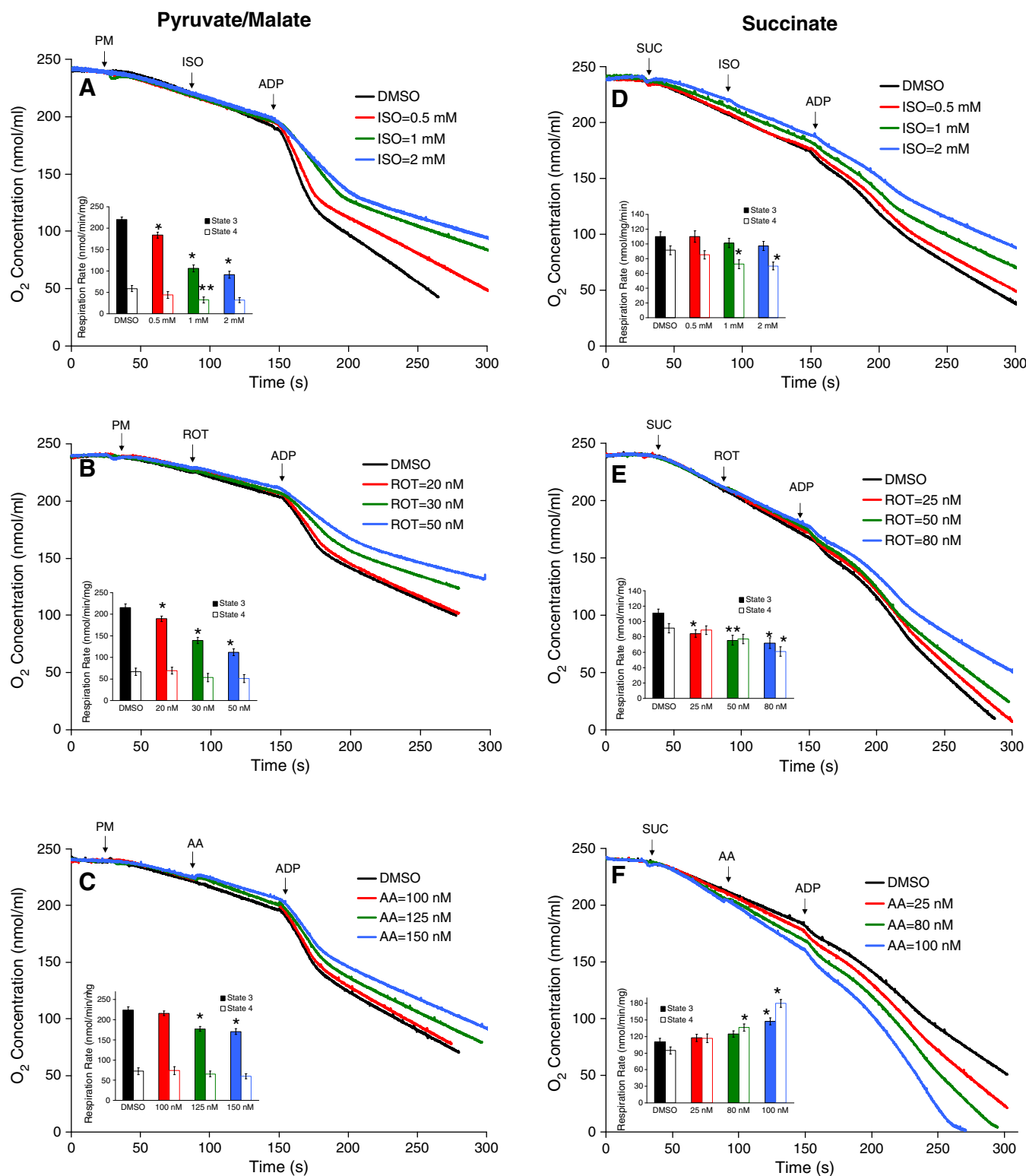


**Fig. 5.** Mitochondrial O<sub>2</sub> concentration (nmol·min<sup>-1</sup>) during states 2, 3 and 4 respiration with different substrates and either ISO or a blocker of ETC complexes. ISO, ROT, or AA was added after PM (A–C) or SUC (D–F) and before ADP. Adding ADP induced a transient depolarization. The insets summarize effects of added ISO, ROT and AA on state 3 and state 4 respiration rates (nmol·min<sup>-1</sup>·mg<sup>-1</sup>protein). Note similarities and differences of responses to each drug. Data represent mean  $\pm$  SD of 3 replicates.

translocation of ADP for ATP. With titrated low concentrations of ATR (150 nM–3  $\mu$ M), there was a concentration dependent decrease in ADP-induced state 3  $\Delta\Psi_m$  depolarization (Fig. 4D); but there was no significant change in the duration of ADP phosphorylation because of lesser exchange of ADP for ATP compared to the DMSO (vehicle) group. The effects of ATR on OxPhos show that ATR incrementally inhibited ANT. The variable responses between ISO and ATR suggested and supported our previous observation that ISO does not have an appreciable effect on ANT activity.

### 3.3. Effect of isoflurane vs. respiratory inhibitors on mitochondrial $O_2$ consumption

Time-dependent effects of DMSO (vehicle) and graded concentrations of ISO, complex I (ROT), or complex III (AA) inhibitors on  $O_2$  consumption rate in the presence of PM or SUC during states 2, 3 and 4 respirations are shown in Fig. 5A–F. The insets show summaries of treatment effects on state 3 and state 4. With the complex I substrate PM, ISO significantly slowed state 3 respiration rate in a concentration-dependent manner:  $183 \pm 7$  (0.5 mM ISO),  $106 \pm 8$  (1 mM ISO), and  $91 \pm 8$  (2 mM ISO) vs.  $220 \pm 6$  (DMSO)  $\text{nmol} \cdot \text{min}^{-1} \cdot \text{mg}^{-1}$  (Fig. 5A inset), with small decreases in state 4 respiration:  $59 \pm 7$  (0.5 mM ISO),  $44 \pm 8$  (1 mM ISO), and  $32 \pm 7$  (2 mM ISO) vs.  $32 \pm 6$  (DMSO)  $\text{nmol} \cdot \text{min}^{-1} \cdot \text{mg}^{-1}$  (Fig. 5A inset). ISO also prolonged the duration of state 3 respiration:  $23 \pm 4$  s,  $40 \pm 6$  s and  $49 \pm 5$  s at 0.5, 1 and 2 mM ISO, respectively, vs.  $21 \pm 6$  s with DMSO. Like ISO, low concentrations of ROT also caused concentration-dependent decreases in respiration and increases in state 3 duration (Fig. 5B). These results are consistent with the effects of ISO and ROT to decrease the magnitude and to increase the duration of NADH oxidation (Fig. 2A,B). Unlike ISO and ROT, AA (in high concentrations) with the substrate PM, caused a slight but significant decrease in respiration rate (Fig. 5C inset) and duration of state 3 (Fig. 5C), which are consistent with the small increases in the duration of state 3 NADH oxidation and  $\Delta\Psi_m$  depolarization (Figs. 2C and 3C).

ISO did not significantly decrease state 3 respiration rate in a concentration-dependent manner with complex II substrate SUC (Fig. 5D). Unlike with the substrate PM, with substrate SUC, ISO decreased state 3 duration:  $63 \pm 7$  s,  $60 \pm 6$  s and  $59 \pm 5$  s at 0.5, 1 and 2 mM ISO, respectively, vs.  $73 \pm 4$  s with DMSO. The effects of ISO with substrate SUC (Fig. 5D) were compared with those of ROT (Fig. 5E) and AA (Fig. 5F). In a concentration-dependent manner, ISO decreased state 4 respiration rate, possibly by inhibiting complex I with attenuation of RET from the reduced Q pool to complex I. The effect

of ISO to decrease state 4 respiration with substrate SUC was again shown to result from attenuated complex I activity because these results were consistent with the effect of ROT to decrease state 4 respiration (Fig. 2 D,E). Unlike ISO, adding AA (at higher concentrations) caused an increase in state 3 respiration compared to DMSO (Fig. 5D vs. F). The effects of ISO, ROT, and AA on concentration-dependent changes in the duration of state 3 respiration showed that responses to ISO closely matched those of ROT with SUC as the substrate (Fig. 5D,E,F).

The effects of ISO and AA on respiration rates with SUC as the substrate after complete block of complex I with high ROT (1  $\mu$ M) were compared (Fig. 6A,B) as was done for  $\Delta\Psi_m$  (Fig. 4A,B). ISO slightly, but significantly, increased state 3 respiration:  $120 \pm 5$  (DMSO),  $128 \pm 7$  (0.5 mM ISO),  $139 \pm 6$  (1 mM ISO) and  $136 \pm 7$  (2 mM ISO)  $\text{nmol} \cdot \text{min}^{-1} \cdot \text{mg}^{-1}$ ; ISO induced a small but significant increase in state 4 respiration. In contrast, AA induced more pronounced increases in state 3 respiration:  $120 \pm 8$  (DMSO),  $228 \pm 8$  (10 nM AA),  $210 \pm 8$  (20 nM AA) and  $213 \pm 1$  (25 nM AA)  $\text{nmol} \cdot \text{min}^{-1} \cdot \text{mg}^{-1}$ . AA also increased state 4 respiration:  $93 \pm 8$  (DMSO),  $133 \pm 6$  (10 nM AA),  $127 \pm 7$  (20 nM AA),  $115 \pm 7$  (25 nM AA)  $\text{nmol} \cdot \text{min}^{-1} \cdot \text{mg}^{-1}$  that could be attributed to electron leak at the inhibited complex III site. Thus, when complex I was completely blocked, electron transfer from complex II to complex IV became attenuated as complex III was step-wise blocked. With blocked proton pumping at complex I and reduced proton pumping at complexes III and IV, this tended to reduce the redox state and  $\Delta\Psi_m$  (Fig. 4A,B), thus stimulating respiration. During state 3 respiration with proton influx at complex V, respiration became even faster until  $\Delta\Psi_m$  was restored.

## 4. Discussion

The mitochondrion has emerged as a key component in VA-mediated cardioprotection against IR injury. VAs (e.g. ISO) could provide cellular protection against IR injury, in part, by direct effects on mitochondrial ETC. complexes or on other proteins (ANT) involved in OxPhos that result in attenuated mitochondrial damage. Prior reports indicate that VAs likely have depressant effects on mitochondrial function [34–36]. However, the specific targets and mechanisms of VA action on mitochondrial respiration and phosphorylation remain to be understood.

The aim of this study was to identify and characterize potential targets of ISO in isolated cardiac mitochondria by monitoring changes in bioenergetic variables (NADH,  $\Delta\Psi_m$ , and respiration) during states 2, 3 and 4 respiration. To do so we used different substrates (PM, SUC,

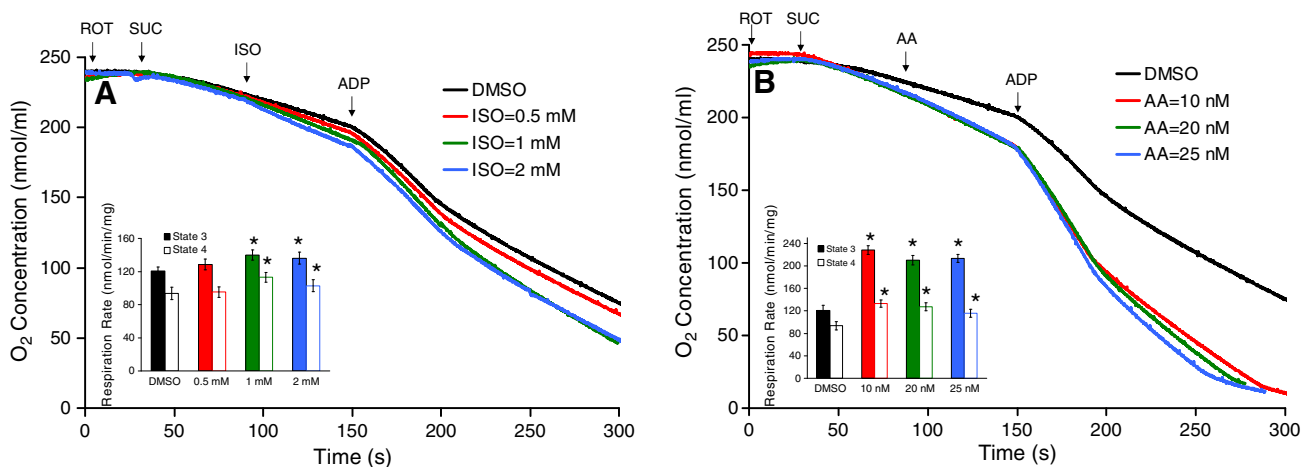


**Fig. 6.** Mitochondrial  $O_2$  concentration ( $\text{nmol} \cdot \text{min}^{-1}$ ) during states 2, 3 and 4 respiration with substrate SUC and either ISO or a blocker (AA) of ETC complexes. ROT (1  $\mu$ M) was given before succinate to maximally block complex I and RET. The insets summarize effects of added ISO, ROT, and AA on state 3 and state 4 respiration rates ( $\text{nmol} \cdot \text{min}^{-1} \cdot \text{mg}^{-1}$  protein). Note similarities and differences of responses to each drug. Data represent mean  $\pm$  SD of 3 replicates.



SUC + ROT) in the absence and presence of ISO to compare its effects with ETC complex inhibitors (ROT, AA, MAL, KCN and OMN) or the ANT inhibitor ATR, each given in ascending submaximal concentrations. Overall, we found that ISO caused concentration-dependent differential modulation of mitochondrial NADH,  $\Delta\Psi_m$ , and respiration under different substrate conditions. Based on the responses and comparisons of ISO and classical ETC inhibitors (Fig. 1) on different states of respiration, we concluded that complex I and complex III are specific respiratory protein targets of ISO by comparing the bioenergetic effects of ISO with those of classical inhibitors. In contrast, using the same approach, our data suggests that ISO does not significantly impair the function of complexes II, IV, V or ANT. The differential modulation of mitochondrial function under different substrate conditions with ISO provides insights into the more or less selective interaction of ISO with mitochondrial proteins. These targets could have significant implications for the mechanism of VA-induced protection against cardiac oxidative stress and could also account, in part, for the mild negative inotropic effect of VA's.

#### 4.1. Isoflurane-induced differential modulation of bioenergetics with substrate PM

Transient NADH oxidation to  $\text{NAD}^+$  during ADP-stimulated respiration is due to a transient decrease in NADH secondary to enhanced proton pumping and electron transfer to replace proton influx via complex V (see Fig. 1). ISO and ROT exhibited very similar effects to attenuate the magnitude and increase the duration of state 3 NADH oxidation (Fig. 2A, B and insets). These effects are likely due to restricted proton pumping by complex I so that proton entry into complex V after adding ADP is slowed and prolonged. The ISO-induced concentration-dependent decreases in NADH oxidation and increases in state 3 NADH duration suggested that ISO attenuates the increases in electron transfer and proton pumping induced by proton influx driven ADP phosphorylation (Fig. 7A); these data were consistent with our previous observation of partial inhibition of complex I by ISO [8]. The low concentrations of ROT (20–80 nM), to mimic the effects of ISO, are believed to partially block electron transfer (and so proton pumping) between the NADH binding site via FeS centers and the Q binding site in complex I. Although we deduced that ISO attenuates complex I function in a similar manner, the concentrations of ISO required to produce the same effect on complex I are about  $10^3$  higher; this may indicate that the potency of ISO for an effect on the Q binding site of complex I is very low or that the molecular mechanism of inhibition on complex I is dissimilar (less specific) from that of ROT. For example, although ROT, like ISO, increased the duration of state 3  $\Delta\Psi_m$  depolarization (Fig. 3A,B), ISO did not change the extent/magnitude of depolarization, whereas ROT increased it substantially. These differential effects on the extent of maximal state 3  $\Delta\Psi_m$  depolarization and NADH oxidation by ISO and ROT appears to imply that ISO attenuated complex I function somewhat differently than ROT. For example, the ISO-induced increase in the duration of ADP phosphorylation is most likely due to attenuation of proton pumping downstream of complex I to better match the slower rates of electron transfer and ADP phosphorylation due to inhibition of the complex. This implies that ISO may have effects other than on complex I only.

ISO, like the complex III  $Q_i$  site inhibitor AA [37–39], increased the duration of state 3  $\Delta\Psi_m$  (Fig. 3A,C) implying that ISO may attenuate complex III in addition to complex I. On the other hand, ISO increased the duration of state 3  $\Delta\Psi_m$  more than AA (Fig. 3A,C). AA and ROT similarly prolonged the duration of state 3  $\Delta\Psi_m$  (Fig. 3B,C) but did not exactly match the effect of ISO (Fig. 3A), which again implicates complex III as another site of ISO action. The ISO and AA-induced increases in duration of ADP phosphorylation most likely result from attenuated proton pumping at complexes III and IV downstream of complex I due to attenuated rates of electron transfer. Note that because ISO appears to simultaneously inhibit complexes I and III, the greater state 3

duration of NADH oxidation and  $\Delta\Psi_m$  depolarization by ISO vs. AA may be due to ISO additionally inhibiting complex I.

The net effect of proton influx at complex V with addition of ADP (Fig. 1) is to temporarily depolarize the IMM and consume NADH as respiration is enhanced to restore the  $\Delta\Psi_m$  and NADH (reducing equivalents). ISO, ROT, and AA each slowed state 3 respiration (Fig. 5A,B,C), presumably because of reduced electron transfer to complex IV associated with decreased proton pumping at complexes I and III. These results extend previous findings [8,23] that suggested that the prolonged duration of state 3 ADP phosphorylation can be attributed to slowed rates of electron transfer and proton pumping by NADH-linked intermediates; this is consistent with the increased duration of state 3 NADH,  $\Delta\Psi_m$ , and respiration with the complex I substrate PM.

A decrease in  $\Delta\Psi_m$  can be caused by any protonophoric effect that would allow ADP-independent influx of protons into the matrix (proton leak) [40,41], which would increase respiration to restore  $\Delta\Psi_m$ . We did not observe any ISO-mediated change in matrix pH with BCECF-AM incubated mitochondria (data not shown), nor any increase in state 2 respiration to support a proton leak (Fig. 5A). Indeed, during respiratory states 3 and 4 ISO slowed the rate of respiration, which is not consistent with a proton leak (Fig. 5A).

A description of FET under these substrate conditions with ISO, ROT, and AA is depicted in Figs. 1 and 7A. We postulate that the mild inhibition of complex I with ROT or ISO decreases the NADH-supported transfer of electrons in the forward direction, i.e. from complex I to complex III and to complex IV, and this results in decreased ADP-induced NADH oxidation and increased state 3 durations of NADH oxidation,  $\Delta\Psi_m$  and respiration. The mild inhibition of complex III with AA or ISO decreases transfer of electrons from complex III to complex IV and this results in an increased duration of state 3  $\Delta\Psi_m$  depolarization, without affecting the magnitude of NADH oxidation (Figs. 2C and 7A).

#### 4.2. Isoflurane-induced differential modulation of bioenergetics with substrate SUC

The complex II substrate (SUC) causes a reversal of the standard reduction potential [25] so that  $\text{NAD}^+$  is reduced to NADH through RET and this causes superoxide generation at complex I [40,42]. Under these conditions ISO and ROT similarly decreased the extent and duration of ADP-induced state 3 NADH oxidation (Fig. 2D,E) and  $\Delta\Psi_m$  depolarization (Fig. 3D,E). These effects resulted from a decreased rate of ADP phosphorylation because the rate of state 3 respiration was actually slower with ISO and ROT (Fig. 5 D,E). A description of slowed FET under these substrate conditions with ISO, ROT or AA is depicted in Fig. 7B. Succinate can generate NADH in complex I through RET, which is sensitive to  $\Delta\Psi_m$  [43]. We interpret from our findings that mild inhibition of complex I with ISO or ROT decreased RET supported generation of NADH and subsequent oxidation of the available NADH resulted in depressed state 3 respiration. The reduced extent and duration of state 3 by ISO or ROT could be attributed to decreased RET-mediated NADH generation and impaired oxidation of NADH due to attenuated complex I function. However, this may not be a major contributing factor since RET may be less favorable when  $\Psi_m$  is depolarized by the added ADP. Therefore, an alternative possibility could be that impaired oxidation of NADH induced by ISO and ROT could lead to a slowing of the TCA cycle activity, thereby leading to accumulation of oxaloacetate, which inhibits complex II. Inhibition of complex II would lead to a decrease in OxPhos capacity with SUC by lowering the  $\Delta\Psi_m$  to result in a decrease in ROS production via oxidation of the ubiquinone pool [44]. A description of slowed FET under these substrate conditions with ISO, ROT and AA is depicted in Fig. 7B.

ISO or ROT-induced decreases in the extent and duration of state 3  $\Delta\Psi_m$  depolarization (Fig. 3 D,E) by attenuation of complex I at the Q site would result in decreased NADH oxidation. The net result would be an increase in reduced NADH and a shorter duration of NADH

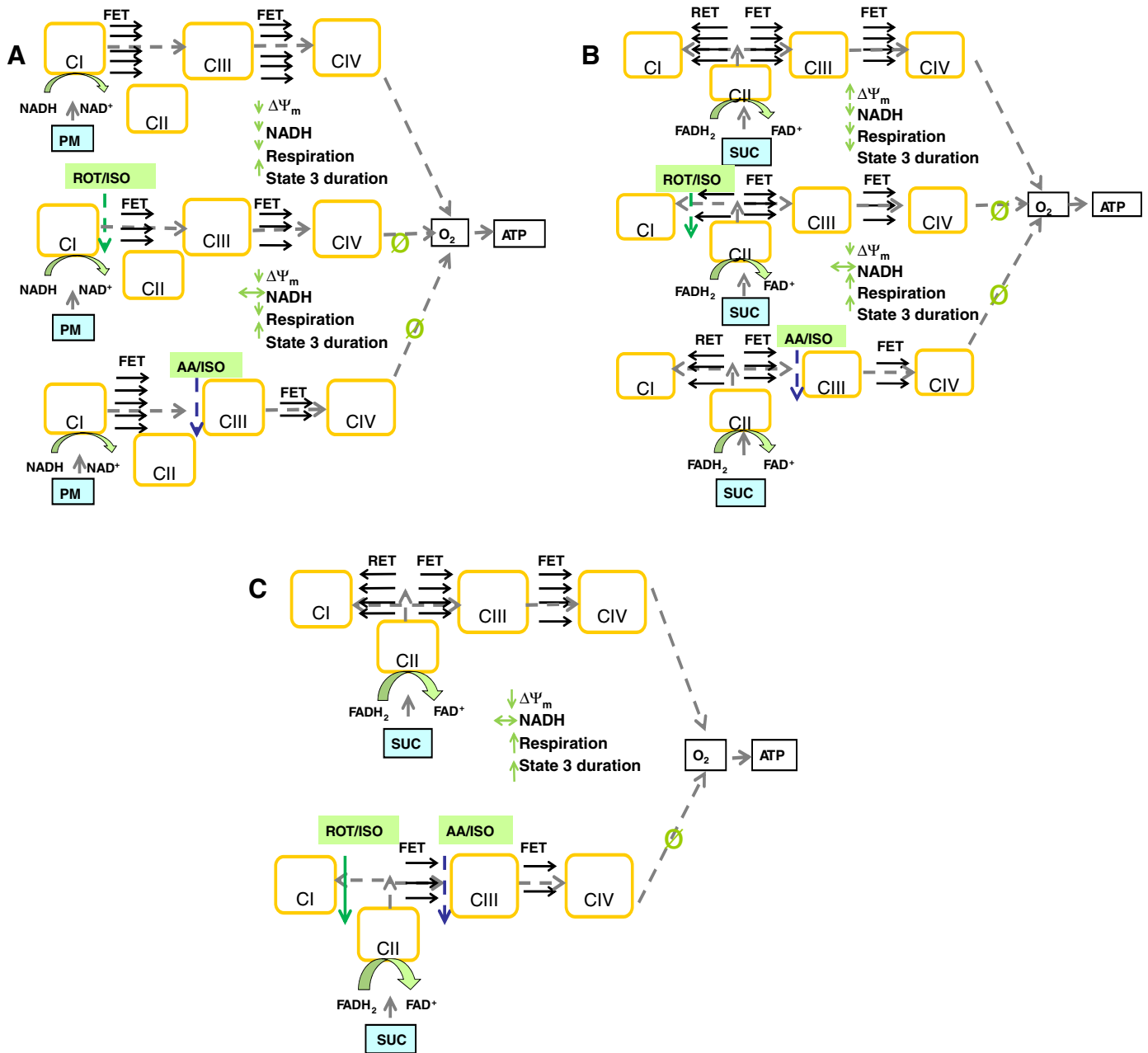


**Fig. 7.** Schema depicting ADP-induced changes in magnitude and duration of mitochondrial bioenergetic variables (NADH,  $\Delta\Psi_m$ , respiration), and presumed changes in electron transfer activity (ETA) along the ETC before and after ISO. ISO is compared with ROT or AA to induce attenuation of complex I and complex III with NAD-linked substrate PM (A), FAD-linked substrate SUC (B), and substrate SUC + ROT after complete inhibition of complex I with 1  $\mu$ M ROT (C). Small arrows ( $\rightarrow$ ) indicate the relative number of electrons transported during FET before and after attenuation of complex I or complex III. Broken arrows ( $\dashrightarrow$ ) near complex I (CI) and complex III (CIII) indicate mild inhibition of complexes and the solid arrow ( $\rightarrow$ ) near complex I indicates complete inhibition of complex I with ROT (1  $\mu$ M). Complexes I–IV (CI–CIV); PM, K<sup>+</sup>-pyruvate/malate; SUC, K<sup>+</sup>-succinate; ISO, isoflurane; ROT, rotenone; AA, antimycin A; FET, forward electron transfer; RET, reverse electron transfer.

oxidation, but decreases in states 3 and 4 respiration (Fig. 5D,E insets). With the substrate PM, unlike the substrate SUC, the ISO-induced increase in duration of state 3 NADH oxidation support inhibition of electron transfer from complex I. However, with the substrate SUC, the marked decreases in the duration of state 3  $\Delta\Psi_m$  depolarization are more likely attributed either to a decrease in FET from the reduced Q site of complex I to the Q pool, or to attenuation of SUC-supported transfer of electrons from complex II by oxaloacetate accumulation. The accumulation of oxaloacetate could result from the inhibitory effect of ROT/ISO to reduce oxidation of NADH during state 3 (Fig. 8). This ISO concentration-dependent effect to decrease state 3 respiration

diminishes the possibility that this is due to blocking complex I electron transfer from the Q pool to complex I or to attenuation of the redox between Q and QH; thus this effect favors the possibility of attenuation in FET along the ETC as depicted in Fig. 8. Moreover, because ISO or ROT depressed state 3 and state 4 respiration with the substrate SUC (Fig. 5D,E), this verifies that ISO and ROT mediated attenuation of complex I function did not lead to an increase in respiration as a result of proton leak at the inhibited complex I. In mitochondria respiring on SUC, the increases in duration of state 3  $\Delta\Psi_m$  depolarization (Fig. 3F) after treatment with AA could occur by impeding electron transfer from the SUC-driven reduced Q pool to complex III.

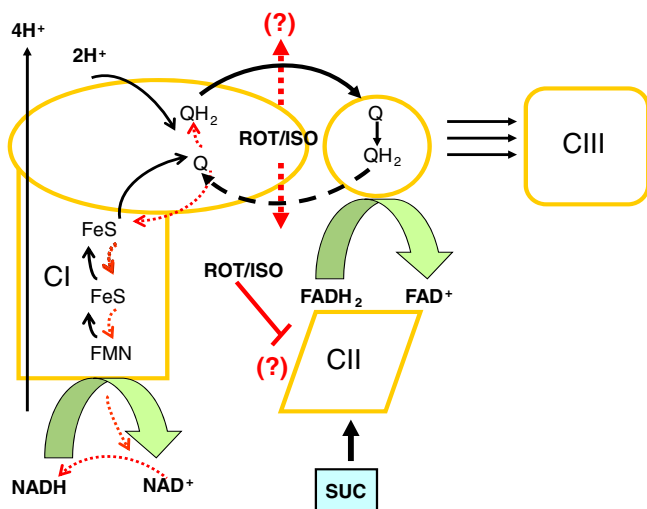


**Fig. 8.** Schema depicting electron transfer from substrate SUC to downstream and upstream complex I and complex III, respectively. Electrons from SUC pass through  $\text{FADH}_2$  to the Q pool, which transfers electrons to the Q site of complex I. Within complex I, electrons transferred to the Q site can either go in the reverse direction via RET through FeS clusters and FMN to generate NADH from  $\text{NAD}^+$  or go in the forward direction via FET to produce  $\text{QH}_2$ ; RET vs. FET is dependent on the standard reduction potential across complex I. Binding of ISO, like ROT, may inhibit the transfer of electrons from the  $\text{QH}_2$  of complex I to the Q pool to complex III. Solid arrows ( $\rightarrow$ ) show electrons transported in the forward direction (FET) and broken arrows ( $\dashrightarrow$ ) show electrons transported in the reverse direction (RET). Question marks (?) show the possible indirect mechanisms of attenuation in FET either via attenuation of electron transfer from the Q site of complex I to the Q pool, or succinate generated accumulation of oxaloacetate due to ROT/ISO mediated decrease in NADH oxidation.

#### 4.3. Isoflurane-induced differential modulation of bioenergetics with substrate SUC and block of complex I

ISO attenuates complex III function, as we deduced in part by the similarity between ISO and AA on increasing the duration of state 3  $\Delta\Psi_m$  depolarization with SUC after completely blocking complex I with 1  $\mu\text{M}$  ROT (Fig. 4A,B). Attenuation of complex III function with inhibited FET and RET at complex I impedes FET from substrate SUC and could lead to electron leak and  $\text{O}_2^-$  generation [25]. The apparent increases in states 3 and 4 respiration with SUC + ROT (Fig. 6A,B) could be attributed to increased  $\text{O}_2^-$  generation, due to electron leak at complex III with AA, rather than reduction of  $\text{O}_2$  to  $\text{H}_2\text{O}$  [45]. The effects of mild inhibition of complex III with ISO or AA to decrease transfer of electrons from complex III to complex IV and to increase the duration of state 3  $\Delta\Psi_m$  depolarization is depicted in Fig. 7C.

We additionally explored the possibility that in the presence of SUC + ROT the ISO-mediated increases in duration of state 3  $\Delta\Psi_m$  depolarization can be alternatively explained by an attenuating effect of ISO on complex II or ANT function. But unlike ISO, which increased the duration of ADP phosphorylation, low concentrations of ATR did not significantly change state 3  $\Delta\Psi_m$  duration (Fig. 4C,D). This implies that ISO-mediated increases in state 3 duration are likely attributed to attenuation of complex III rather than to attenuation of complex II function or attenuation of transfer of ADP/ATP by ANT. The data obtained on attenuation of complex IV function by KCN (data not shown), and its comparison by ISO, suggests that complex IV is also not a potential target of ISO.

Because ISO induced small increases in states 2, 3, and 4 respiration (Fig. 6A) under the substrate SUC + ROT (1  $\mu\text{M}$ ), we tested if ISO exhibited characteristics of proton leak (uncoupling) by comparing the effects of low titrated concentrations of known uncouplers (DNP, FCCP) to induce mitochondrial  $\Delta\Psi_m$  depolarization. Compared to ISO, these uncoupling agents caused a pronounced state 2 depolarization (data not shown). In addition, matrix acidification and  $\Delta\Psi_m$  depolarization

are hallmarks of proton leak [41,46], but we did not observe any change in matrix pH measured by BCECF fluorescence (data not shown).

#### 4.4. Isoflurane-induced effects on complexes I and III: implication for cardioprotection

Volatile anesthetics protect the myocardium against IR injury, in part, by modulating mitochondrial respiratory function [47–49] to mildly disrupt electron transfer and induce small amount of ROS, which acts as a signaling molecule [11,18,33,35]. In this current study, we concentrated on identifying the direct effects of ISO on proteins involved in mitochondrial respiration, nucleotide transfer and OxPhos with the aim to better understand how VAs modulate cardiac function and confer protection against IR injury.

We proposed that ISO-mediated cardioprotection is initiated by partial inhibition of at least several ETC protein components to cause decreased electron transport and induce ROS production, which in turn initiates cardioprotective pathways. Based on this and prior studies, we believe it is plausible that ISO protects by attenuating complex I and complex III activity to cause 1) release of small amounts of ROS at complex I [50–52] and complex III [53,54] during the period before ischemia (APC) or after ischemia (APOC), and 2) decrease in  $\text{O}_2$  consumption by reducing the workload during the period of limited  $\text{O}_2$  availability during ischemia [55]. These events could limit deleterious ROS generation during IR and so prevent mitochondria from initiating apoptotic events leading to cell death. We showed previously that limiting complex I activity during ischemia has the potential to minimize accumulation of ROS on reperfusion and therefore to protect mitochondria and the cell from oxidative damage [19].

Notably, both complex I and complex III are targets but also sites of ROS generation [45,56,57]. The cardioprotective effect of ISO against IR injury could also be triggered by a small rise in ROS by its selective inhibition of ETC activity at complex I [50–52] and complex III [53,54]. Our study provides useful information on effects of ISO on forward and backward electron transfer pathways that modulate mitochondrial bioenergetics in a way that may contribute to cardioprotection.

#### Acknowledgements

This work was supported by the National Institute of Health Grants P01-GM066730 (ZJB), R01-HL095122 (AKSC and RKD) and R01-HL089514 (DFS).

#### References

- [1] E. Murphy, C. Steenbergen, Mechanisms underlying acute protection from cardiac ischemia–reperfusion injury, *Physiol. Rev.* 88 (2008) 581–609.
- [2] Q. Chen, A.K. Camara, D.F. Stowe, C.L. Hoppel, E.J. Lesnfsky, Modulation of electron transport protects cardiac mitochondria and decreases myocardial injury during ischemia and reperfusion, *Am. J. Physiol. Cell Physiol.* 292 (2007) C137–C147.
- [3] A.K. Camara, M. Bienengraeber, D.F. Stowe, Mitochondrial approaches to protect against cardiac ischemia and reperfusion injury, *Front. Physiol.* 2 (2011) 13.
- [4] J.S. Armstrong, Mitochondria-directed therapeutics, *Antioxid. Redox Signal.* 10 (2008) 575–578.
- [5] D. Pradvic, Y. Mio, F. Sedlic, P.F. Pratt, D.C. Warltier, Z.J. Bosnjak, M. Bienengraeber, Isoflurane protects cardiomyocytes and mitochondria by immediate and cytosol-independent action at reperfusion, *Br. J. Pharmacol.* 160 (2010) 220–232.
- [6] A. Stadnicka, J. Marinovic, M. Ljubkovic, M.W. Bienengraeber, Z.J. Bosnjak, Volatile anesthetic-induced cardiac preconditioning, *J. Anesth.* 21 (2007) 212–219.
- [7] N.R. Van Allen, P.R. Krafft, A.S. Leitzke, R.L. Applegate Jr, J. Tang, J.H. Zhang, The role of volatile anesthetics in cardioprotection: a systematic review, *Med. Gas Res.* 2 (2012) 22.
- [8] B. Agarwal, A.K. Camara, D.F. Stowe, Z.J. Bosnjak, R.K. Dash, Enhanced charge-independent mitochondrial free  $\text{Ca}^{2+}$  and attenuated ADP-induced NADH oxidation by isoflurane: implications for cardioprotection, *Biochim. Biophys. Acta* 1817 (2012) 453–465.
- [9] K. Tanaka, L.M. Ludwig, J.R. Kersten, P.S. Pagel, D.C. Warltier, Mechanisms of cardioprotection by volatile anesthetics, *Anesthesiology* 100 (2004) 707–721.
- [10] D.F. Stowe, L.G. Kevin, Cardiac preconditioning by volatile anesthetic agents: a defining role for altered mitochondrial bioenergetics, *Antioxid. Redox Signal.* 6 (2004) 439–448.

- [11] M. Zaugg, M.C. Schaub, Signaling and cellular mechanisms in cardiac protection by ischemic and pharmacological preconditioning, *J. Muscle Res. Cell Motil.* 24 (2003) 219–249.
- [12] M.L. Riess, D.F. Stowe, D.C. Warltier, Cardiac pharmacological preconditioning with volatile anesthetics: from bench to bedside? *Am. J. Physiol. Heart Circ. Physiol.* 286 (2004) H1603–H1607.
- [13] Z.D. Ge, D. Pravdic, M. Bienengraeber, P.F. Pratt Jr., J.A. Auchampach, G.J. Gross, J.R. Kersten, D.C. Warltier, Isoflurane postconditioning protects against reperfusion injury by preventing mitochondrial permeability transition by an endothelial nitric oxide synthase-dependent mechanism, *Anesthesiology* 112 (2010) 73–85.
- [14] P.S. Pagel, Postconditioning by volatile anesthetics: salvaging ischemic myocardium at reperfusion by activation of prosurvival signaling, *J. Cardiothorac. Vasc. Anesth.* 22 (2008) 753–765.
- [15] R. Bains, M.C. Moe, G.A. Larsen, J. Berg-Johnsen, M.L. Vinje, Volatile anaesthetics depolarize neural mitochondria by inhibition of the electron transport chain, *Acta Anaesthesiol. Scand.* 50 (2006) 572–579.
- [16] M.L. Riess, A.K. Camara, Q. Chen, E. Novalija, S.S. Rhodes, D.F. Stowe, Altered NADH and improved function by anesthetic and ischemic preconditioning in guinea pig intact hearts, *Am. J. Physiol. Heart Circ. Physiol.* 283 (2002) H53–H60.
- [17] L.G. Kevin, E. Novalija, M.L. Riess, A.K. Camara, S.S. Rhodes, D.F. Stowe, Sevoflurane exposure generates superoxide but leads to decreased superoxide during ischemia and reperfusion in isolated hearts, *Anesth. Analg.* 96 (2003) 949–955 (table of contents).
- [18] M.L. Riess, L.G. Kevin, J. McCormick, M.T. Jiang, S.S. Rhodes, D.F. Stowe, Anesthetic preconditioning: the role of free radicals in sevoflurane-induced attenuation of mitochondrial electron transport in Guinea pig isolated hearts, *Anesth. Analg.* 100 (2005) 46–53.
- [19] M. Aldakkak, D.F. Stowe, Q. Chen, E.J. Lesnefsky, A.K. Camara, Inhibited mitochondrial respiration by amobarbital during cardiac ischaemia improves redox state and reduces matrix  $\text{Ca}^{2+}$  overload and ROS release, *Cardiovasc. Res.* 77 (2008) 406–415.
- [20] L.S. Burwell, S.M. Nadtochiy, P.S. Brookes, Cardioprotection by metabolic shut-down and gradual wake-up, *J. Mol. Cell. Cardiol.* 46 (2009) 804–810.
- [21] P.J. Cohen, Effect of anesthetics on mitochondrial function, *Anesthesiology* 39 (1973) 153–164.
- [22] M.L. Nahrwold, P.J. Cohen, Anesthetics and mitochondrial respiration, *Clin. Anesth.* 11 (1975) 25–44.
- [23] P.J. Hanley, J. Ray, U. Brandt, J. Daut, Halothane, isoflurane and sevoflurane inhibit NADH:ubiquinone oxidoreductase (complex I) of cardiac mitochondria, *J. Physiol.* 544 (2002) 687–693.
- [24] F. Sedlic, D. Pravdic, N. Hirata, Y. Mio, A. Sepac, A.K. Camara, T. Wakatsuki, Z.J. Bosnjak, M. Bienengraeber, Monitoring mitochondrial electron fluxes using NAD(P)H-flavoprotein fluorometry reveals complex action of isoflurane on cardiomyocytes, *Biochim. Biophys. Acta* 1797 (2010) 1749–1758.
- [25] D.F. Stowe, A.K. Camara, Mitochondrial reactive oxygen species production in excitable cells: modulators of mitochondrial and cell function, *Antioxid. Redox Signal.* 11 (2009) 1373–1414.
- [26] M.M. Bradford, A rapid and sensitive method for the quantitation of microgram quantities of protein utilizing the principle of protein–dye binding, *Anal. Biochem.* 72 (1976) 248–254.
- [27] M. Aldakkak, D.F. Stowe, R.K. Dash, A.K. Camara, Mitochondrial handling of excess  $\text{Ca}^{2+}$  is substrate-dependent with implications for reactive oxygen species generation, *Free Radic. Biol. Med.* 56 (2013) 193–203.
- [28] A.D. Boelens, R.K. Pradhan, C.A. Blomeyer, A.K. Camara, R.K. Dash, D.F. Stowe, Extra-matrix  $\text{Mg}^{(2+)}$  limits  $\text{Ca}^{(2+)}$  uptake and modulates  $\text{Ca}^{(2+)}$  uptake-independent respiration and redox state in cardiac isolated mitochondria, *J. Bioenerg. Biomembr.* 45 (2013) 203–218.
- [29] C.A. Blomeyer, J.N. Bazil, D.F. Stowe, R.K. Pradhan, R.K. Dash, A.K. Camara, Dynamic buffering of mitochondrial  $\text{Ca}^{(2+)}$  during  $\text{Ca}^{(2+)}$  uptake and  $\text{Na}^{(+)}$ -induced  $\text{Ca}^{(2+)}$  release, *J. Bioenerg. Biomembr.* 45 (2013) 189–202.
- [30] J. Haumann, R.K. Dash, D.F. Stowe, A.D. Boelens, D.A. Beard, A.K. Camara, Mitochondrial free  $[\text{Ca}^{2+}]$  increases during ATP/ADP antiport and ADP phosphorylation: exploration of mechanisms, *Biophys. J.* 99 (2010) 997–1006.
- [31] R.C. Scaduto Jr., L.W. Grotyohann, Measurement of mitochondrial membrane potential using fluorescent rhodamine derivatives, *Biophys. J.* 76 (1999) 469–477.
- [32] A. Heinen, M. Aldakkak, D.F. Stowe, S.S. Rhodes, M.L. Riess, S.G. Varadarajan, A.K. Camara, Reverse electron flow-induced ROS production is attenuated by activation of mitochondrial  $\text{Ca}^{2+}$ -sensitive  $\text{K}^{+}$  channels, *Am. J. Physiol. Heart Circ. Physiol.* 293 (2007) H1400–H1407.
- [33] A. Heinen, A.K. Camara, M. Aldakkak, S.S. Rhodes, M.L. Riess, D.F. Stowe, Mitochondrial  $\text{Ca}^{2+}$ -induced  $\text{K}^{+}$  influx increases respiration and enhances ROS production while maintaining membrane potential, *Am. J. Physiol. Cell Physiol.* 292 (2007) C148–C156.
- [34] S.M. Nadtochiy, L.S. Burwell, P.S. Brookes, Cardioprotection and mitochondrial S-nitrosation: effects of S-nitroso-2-mercapto-propionyl glycine (SNO-MPG) in cardiac ischemia–reperfusion injury, *J. Mol. Cell. Cardiol.* 42 (2007) 812–825.
- [35] E.J. Lesnefsky, Q. Chen, S. Moghaddas, M.O. Hassan, B. Tandler, C.L. Hoppel, Blockade of electron transport during ischemia protects cardiac mitochondria, *J. Biol. Chem.* 279 (2004) 47961–47967.
- [36] M. Shlafer, C.L. Myers, S. Adkins, Mitochondrial hydrogen peroxide generation and activities of glutathione peroxidase and superoxide dismutase following global ischemia, *J. Mol. Cell. Cardiol.* 19 (1987) 1195–1206.
- [37] B. Lai, L. Zhang, L.Y. Dong, Y.H. Zhu, F.Y. Sun, P. Zheng, Inhibition of Qi site of mitochondrial complex III with antimycin A decreases persistent and transient sodium currents via reactive oxygen species and protein kinase C in rat hippocampal CA1 cells, *Exp. Neurol.* 194 (2005) 484–494.
- [38] X. Gao, X. Wen, L. Esser, B. Quinn, L. Yu, C.A. Yu, D. Xia, Structural basis for the quinone reduction in the bc1 complex: a comparative analysis of crystal structures of mitochondrial cytochrome bc1 with bound substrate and inhibitors at the Qi site, *Biochemistry* 42 (2003) 9067–9080.
- [39] J.S. Armstrong, H. Yang, W. Duan, M. Whiteman, Cytochrome bc1 regulates the mitochondrial permeability transition by two distinct pathways, *J. Biol. Chem.* 279 (2004) 50420–50428.
- [40] A.J. Lambert, M.D. Brand, Superoxide production by NADH:ubiquinone oxidoreductase (complex I) depends on the pH gradient across the mitochondrial inner membrane, *Biochem. J.* 382 (2004) 511–517.
- [41] D. Pravdic, N. Hirata, L. Barber, F. Sedlic, Z.J. Bosnjak, M. Bienengraeber, Complex I and ATP synthase mediate membrane depolarization and matrix acidification by isoflurane in mitochondria, *Eur. J. Pharmacol.* 690 (2012) 149–157.
- [42] J.R. Treberg, C.L. Quinlan, M.D. Brand, Evidence for two sites of superoxide production by mitochondrial NADH-ubiquinone oxidoreductase (complex I), *J. Biol. Chem.* 286 (2011) 27103–27110.
- [43] Y. Liu, G. Fiskum, D. Schubert, Generation of reactive oxygen species by the mitochondrial electron transport chain, *J. Neurochem.* 80 (2002) 780–787.
- [44] S. Drose, L. Bleier, U. Brandt, A common mechanism links differently acting complex II inhibitors to cardioprotection: modulation of mitochondrial reactive oxygen species production, *Mol. Pharmacol.* 79 (2011) 814–822.
- [45] Q. Chen, S. Moghaddas, C.L. Hoppel, E.J. Lesnefsky, Ischemic defects in the electron transport chain increase the production of reactive oxygen species from isolated rat heart mitochondria, *Am. J. Physiol. Cell Physiol.* 294 (2008) C460–C466.
- [46] S.M. Nadtochiy, A.J. Tompkins, P.S. Brookes, Different mechanisms of mitochondrial proton leak in ischaemia/reperfusion injury and preconditioning: implications for pathology and cardioprotection, *Biochem. J.* 395 (2006) 611–618.
- [47] C. Steenbergen, M.E. Perlman, R.E. London, E. Murphy, Mechanism of preconditioning. Ionic alterations, *Circ. Res.* 72 (1993) 112–125.
- [48] A.K. Camara, E.J. Lesnefsky, D.F. Stowe, Potential therapeutic benefits of strategies directed to mitochondria, *Antioxid. Redox Signal.* 13 (2010) 279–347.
- [49] M. Zaugg, E. Lucchinetti, M. Uecker, T. Pasch, M.C. Schaub, Anaesthetics and cardiac preconditioning. Part I. Signalling and cytoprotective mechanisms, *Br. J. Anaesth.* 91 (2003) 551–565.
- [50] M.L. Riess, J.T. Eells, L.G. Kevin, A.K. Camara, M.M. Henry, D.F. Stowe, Attenuation of mitochondrial respiration by sevoflurane in isolated cardiac mitochondria is mediated in part by reactive oxygen species, *Anesthesiology* 100 (2004) 498–505.
- [51] G. Paradies, G. Petrosillo, M. Pistolesi, F.M. Ruggiero, Reactive oxygen species affect mitochondrial electron transport complex I activity through oxidative cardiolipin damage, *Gene* 286 (2002) 135–141.
- [52] L.B. Becker, New concepts in reactive oxygen species and cardiovascular reperfusion physiology, *Cardiovasc. Res.* 61 (2004) 461–470.
- [53] Q. Chen, E.J. Vazquez, S. Moghaddas, C.L. Hoppel, E.J. Lesnefsky, Production of reactive oxygen species by mitochondria: central role of complex III, *J. Biol. Chem.* 278 (2003) 36027–36031.
- [54] T.V. Votyakova, I.J. Reynolds, DeltaPsi(m)-dependent and -independent production of reactive oxygen species by rat brain mitochondria, *J. Neurochem.* 79 (2001) 266–277.
- [55] B.W. Palmisano, R.W. Mehner, D.F. Stowe, Z.J. Bosnjak, J.P. Kampine, Direct myocardial effects of halothane and isoflurane. Comparison between adult and infant rabbits, *Anesthesiology* 81 (1994) 718–729.
- [56] V.G. Grivennikova, A.D. Vinogradov, Partitioning of superoxide and hydrogen peroxide production by mitochondrial respiratory complex I, *Biochim. Biophys. Acta* 1827 (2013) 446–454.
- [57] N. Hirata, Y.H. Shim, D. Pravdic, N.L. Lohr, P.F. Pratt Jr., D. Weihrauch, J.R. Kersten, D.C. Warltier, Z.J. Bosnjak, M. Bienengraeber, Isoflurane differentially modulates mitochondrial reactive oxygen species production via forward versus reverse electron transport flow: implications for preconditioning, *Anesthesiology* 115 (2011) 531–540.